Journal of Hydrology 502 (2013) 191–201

Contents lists available at ScienceDirect

Journal of Hydrology

journal homepage: www.elsevier.com/locate/jhydrol

Flood magnitudes in the Tagus River (Iberian Peninsula) and its stochastic relationship with daily North Atlantic Oscillation since mid-19th Century

Ana Rita Salgueiro [a], Maria J. Machado [b], Mariano Barriendos [c], Henrique Garcia Pereira [d], Gerardo Benito [b,*]

[a] GeoBioTec/Dep. Geociências, Universidade de Aveiro, 3810-193 Aveiro, Portugal
[b] Museo Nacional de Ciencias Naturales, CSIC, Serrano 115 bis, 28006 Madrid, Spain
[c] Departament D'Història Moderna, Universitat de Barcelona, 08001 Barcelona, Spain
[d] Cerena/DECivil, Instituto Superior Técnico, Universidade Técnica de Lisboa, Portugal

ARTICLE INFO

Article history:
Received 22 February 2013
Received in revised form 2 August 2013
Accepted 5 August 2013
Available online 24 August 2013
This manuscript was handled by Andras Bardossy, Editor-in-Chief, with the assistance of Niko Verhoest, Associate Editor

Keywords:
Floods
North Atlantic Oscillation
Qualitative regression
Correspondence Analysis
Tagus River
Iberian Peninsula

SUMMARY

This paper presents a new methodological approach in the analysis of the influence of the North Atlantic circulation on the flood magnitude of the Tagus River, the largest Atlantic draining river of the Iberian Peninsula. This methodology is based on Correspondence Analysis viewed as a qualitative regression tool. A daily scale database (sea level atmospheric pressure, river discharge, rainfall) was used for this study. The selected streamflow station, Vila Velha de Rodão (Portugal, near the Spanish border), holds the longest continuous daily river discharge register of the Iberian Peninsula (over 160 years, since 1852). The annual maximum flood magnitudes were classified into seven categories according to their specific recurrence intervals (T). The qualitative regression approach was used to relate annual peak flood occurrence with the North Atlantic Oscillation (NAO) index mode (positive or negative) registered, during the preceding 40 days (divided in 8 successive 5-day periods). Large floods (categories 1–2 of $T > 50$ years and category 3, $T \sim 25$–50 years) were found to be associated with a very high frequency of the negative NAO mode during the initial 20–25 days (within a total 40 days period length) before de flood peak. The lack of significant association of these flood categories with a predominant NAO mode during the immediately preceding 15 days, prior to the flood, suggest a time lag of 15 days before the peak. Minor flooding (category 7, $T < 2$ years) show a high degree of association with the presence of a positive NAO mode during the previous 20–25 days. The analysis of flood response under natural and dam-regulated regimes (before and after the construction of dams ca 1960) revealed no changes in the behaviour of major floods (responding to a period of 25 days with a dominant negative NAO index mode). Moderate flooding of category 4 (T: 10–25 years), that during the pre-dam construction period were linked to the existence of an initial 5–15 days of negative NAO mode, were not documented during the post-dam period, probably due to flood peak discharge attenuation by reservoirs. The clear climatic control (rainfall accumulation and number of persisting NAO negative mode days) in the onset of flood category 3 (T: 25–50 years) was also statistically blurred during the post-dam period, due to the effective role of dam operation in flood management during wet winters. This dam management effect does not seem to mask the meteorologically related largest flood magnitude events ($T > 50$ years), indicating that catastrophic events will likely occur under the NAO negative daily and seasonal patterns defined in this work. The robustness of the model was assessed by the phenomenological analysis of misclassified Flood/NAO events. Results also indicate that flood management practises may benefit from improved climate scenarios and forecasting of the NAO index.

1. Introduction

The Iberia Peninsula is located in the southern rim of the Atlantic zonal circulation, which confers a particular susceptibility to inter-annual shifts in the trajectory of frontal systems (Capel, 1981; Trigo and Palutikof, 2001). When there is a low zonal circulation over the Atlantic (at 35–40°N), the successive passage of frontal systems from west to east produces continuous and persistent daily precipitation, particularly in the western part of the Iberian Peninsula. This circulation pattern occurs more frequently during winter, and rainfall distribution over the Peninsula depends on the wind trajectory (SW, W or NW) and the local orographic effects (Goodess and Jones, 2002; Cortesi et al., 2012). The North Atlantic Oscillation (NAO) is an index of the dominant pattern of the sea-le-

* Corresponding author. Tel.: +34 917452500x980606; fax: +34 915640800.
E-mail address: benito@mncn.csic.es (G. Benito).

0022-1694/$ - see front matter © 2013 Elsevier B.V. All rights reserved.
http://dx.doi.org/10.1016/j.jhydrol.2013.08.008

vel pressure variations between the Icelandic low and the Azores high, with a low (negative) index being associated to suppressed westerlies and storm track moving southerly toward the Mediterranean Sea (Walker and Bliss 1932; van Loon and Rogers 1978). Recent studies on the influence of the North Atlantic Oscillation (NAO) in the Iberian Peninsula precipitation patterns demonstrate the correlation between periods of NAO in negative mode with humid/wet conditions (Corte-Real et al., 1998; Rodó et al., 1997; González-Rouco et al., 2000; Trigo and Palutikof, 2001). The strong correlation of NAO negative (positive) mode with precipitation above (below) average is likely to influence rainfall sensitive natural systems (e.g. hydrological, ecological) and anthropogenic activities (Hurrell et al., 2003; Vicente-Serrano and Trigo, 2011), including impacts on water resources (e.g. Trigo et al., 2004; López-Moreno et al., 2007; Morán-Tejeda et al., 2011). In general, these studies show that river flow tends to be lower when the NAO index is in its positive phase and higher when under influence of negative NAO. However, the orographic characteristics of the Iberian Peninsula that influence precipitation intensity and type (snow vs. rainfall) at a regional scale, together with drainage basins diversity (land-use, vegetation, stream gradient, etc.) are responsible for a variety of different relationships between NAO and rainfall/flood magnitude (Paredes et al., 2006; Trigo et al., 2008; Trigo, 2011; Lorenzo-Lacruz et al., 2011). At a monthly resolution, the response of river discharge and reservoir storage to late winter (JFM) rainfall patterns related to positive or negative NAO phases shows a 1-month lag time response (Trigo, 2011).

Flooding of major Iberian rivers draining towards the Atlantic is mainly related to persistent rainfall (several weeks) caused by the successive passage of Atlantic cold fronts over the Iberian Peninsula during winter. It is, therefore, expected a strong impact of the NAO on the occurrence of extreme flooding in large Atlantic rivers (e.g. Guadalquivir, Guadiana, Tagus, Douro). In the Tagus River, Benito et al. (2008) found a good correlation between negative average winter (DJF – December/January/February) NAO index and maximum peak discharges recorded during those months from instrumental (gauge stations) and documentary sources. The link between the winter NAO index and extreme floods can also be detected in certain episodes obtained through historic documents for the basins of the Guadalquivir (Benito et al., 2005) and Guadiana (Ortega and Garzón, 2004), as well as a correlation between some flood periods and moments of maximum solar activity (Benito et al., 2003a,b, 2004; Vaquero, 2004). Nevertheless, it was also noticed (Benito et al., 2008) that the existence of negative winter (DJF) NAO index values was not always associated with the occurrence of extraordinary floods. Most studies linking NAO index with floods (Benito et al., 2008; Machado et al., 2011; Silva et al., 2012) have used seasonal and monthly correlations leading to lack of significant connection and/or a delayed response between oscillation mode and hydrological event. Floods are produced by rainfall excess with an immediate hydrological response, requiring therefore a detailed analysis of NAO index at daily resolution.

In this paper, a novel methodological approach is proposed to analyse the relationship between daily NAO mode and the magnitude of the maximum annual flood in a large Iberian river (Tagus River). The use of the Correspondence Analysis as a qualitative regression tool is able to associate the frequency of positive and negative NAO index values, at a daily scale, with flood magnitude, previously converted into a qualitative ordinal variable. Based on this new methodological approach, the aim of this study is to characterize flood magnitude in relation to daily NAO index variability, as a way to understanding flood response to climate change, and to improve the use of NAO patterns as a predicting tool in flood management. The specific objectives of the paper are to: (1) analyse the daily NAO index sequences leading to flooding, (2) provide connections between flood magnitude and NAO patterns, (3) analyse how dam constructions have enhanced and/or attenuate flood response to NAO.

2. Hydro-climatic data source

Two main criteria were used in the selection of streamflow and rainfall stations within the Tagus river basin: their representativeness in terms of reflecting the general stream flood regime within the basin, and the quality and length of the gauge record. Vila Velha de Rodão (Portugal) was the only streamflow station to fulfil all the criteria with a continuous instrumental record of 160 years (source: INAG – Portuguese Water Agency). This record consists of hydrometric observations (four times per day) until 1900, and continuous hydrometric records until 1980 (Fig. 1). The record was completed and cross-checked for data robustness with the gauge records of Alcantara and Cedillo (Spanish Tagus River Water Authority) and downstream gauge record at Omnios (Portugal). The record of Annual Maximum Floods (AMF) was divided into seven flood categories according to peak discharge ranges representing average recurrence intervals (Table 1). Table 1 was derived from flood frequency analysis of combined annual flood data (period 1900–2001) and historic floods (1852–1899) fitted to a Two Components Extreme Value distribution function (Rossi et al., 1984) using the Maximum Likelihood Estimation (MLE) method (Frances et al., 1994).

Rainfall data from stations with long rainfall records, was collected and assessed for their quality (instrumental gaps, record size, record inaccuracies and record sensitivity to rainfall derived from the successive passage of Atlantic cold fronts during winter) and compared with different climatological data series (Santarém in Portugal, Badajoz and Talavera de la Reina in Spain). Badajoz was selected as the rainfall reference station, with over 147 years of continuous precipitation daily records (source: Spanish Agency of Meteorology AEMET). After a quality control checking, anomalous records were detected in early recording years (1864–1876) and therefore not considered in the analysis of extreme rainfall events.

Data on the position of zonal circulation over the Iberian Peninsula is given by records of the positive/negative phase of the North Atlantic Oscillation index (NAO) at a daily resolution. The NAO index during the period 2000–2007 was obtained from NOAA (http://www.cpc.ncep.noaa.gov). In this study, daily values of NAO index for the period between 1820 and 2000 were calculated from the standardised difference in pressure at sea level between San Fernando-Cádiz (Spain) and Reykjavik (Iceland). The San Fernando-Cádiz record was collected from original meteorological observations preserved in historical archives and yearly publications of San Fernando Spanish Navy Observatory (Barriendos et al., 2002), whereas the Reykjavik record was supplied by the Icelandic Meterological Office. Floods, precipitation and NAO index data were cross-checked for a total of 113 cases of AMF (from 1876 to 2007, being all years represented since 1900).

3. Identifying floods/NAO relationships – a novel approach using Correspondence Analysis

3.1. Database construction

In this approach, the statistical unit to which variables refer to is the Annual Maximum Flood (AMF), which, in the case of the Tagus River, covers a continuous hydrological data period between 1876 and 2007. Each event is labelled by its date of occurrence (year/month) and it is characterized by three sets of variables: (i) the daily NAO for the period of 40 days before the event, (ii) the daily rainfall (mm) recorded for the same period, and (iii) the mag-

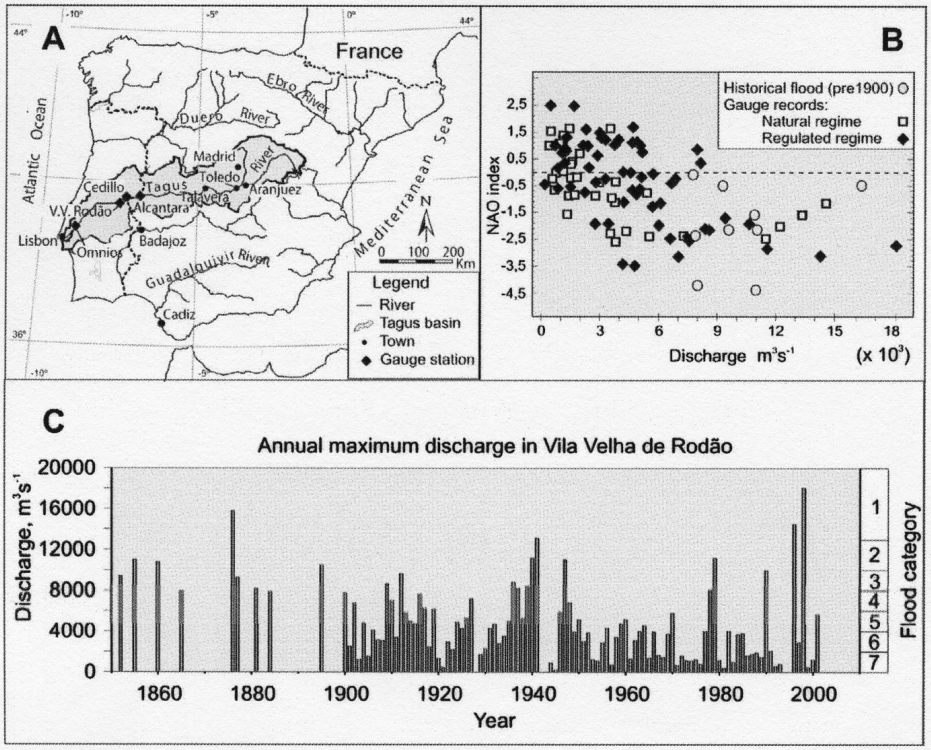

Fig. 1. The Tagus River Basin in the Iberian Peninsula. (A) Location of the historical and instrumental records used; (B) relationship between the annual flood peak discharge at Vila Velha de Rodão and the corresponding month value of NAO index. Discharges over 8000 $m^3 s^{-1}$ are always related with negative NAO phase; and (C) annual maximum flood series in the Vila Velha de Rodão gauge station, with vertical bars showing the peak discharge and the equivalent flood category used in the correspondence analysis.

Table 1
Flood Magnitude categories, peak discharge and associated recurrence interval (T). Flood categories and flood index (FI) numbers are used in the data model contingency tables (Figs. 2 and 9). Categories 1 and 2 where merged in the CA analysis (FI12).

Flood index (FI)	Flood category	Average recurrence interval (T in years)	Discharge ($m^3 s^{-1}$)
1	Centennial	>100	>13000
2	Rare	50–100	10000–13000
3	Exceptional	25–50	8000–10000
4	Extraordinary	10–25	6000–8000
5	Occasional	5–10	4000–6000
6	Ordinary	2–5	2000–4000
7	Minor	<2	<2000

nitude of the flood, converted into an ordinal scale, with seven categories.

If the entire available data base is to be treated by a coherent stochastic methodology, attention should be paid to the severe contrast in accuracy between recent series and early ones (for example, those referring to the 19th century). When both types of data are to be dealt with jointly by the same model in order to take benefit from the sample range over a large time span (1852–2007), classical regression methods based on quantitative variables can lead to misleading results, because such methods do not account for accuracy disproportion. This drawback is particularly critical for the NAO quantitative value, obtained by accurate instrumental techniques in recent years, in contrast to the less precise and more random atmospheric pressure readings available in early years. The case can be made that the maximum common reliable information that can be drawn from the entire NAO data base is the qualitative variable referring to the NAO sign. In this context, the NAO data can account only for the frequency of NAO mode – expressed by its positive and negative modality – in a given period. This calls for viewing the NAO block as a concatenation of contingency tables, each one of which provides the counts, along the entire range of the years (1852–2007), of the two NAO modalities for successive lags. Obviously, when NAO is converted into contingency tables, the other variables, namely AMF, should be also put in the same qualitative format, which entails that non-linear relationships can be revealed. It is arguable that the 'loss of information' involved in this procedure is a minor disadvantage, when compared with the misinterpretation that can emerge from improper quantitative linear multivariate regression models – this argument follows Keynes' famous dictum: "It is better to be roughly right than precisely wrong" –.

Given the above outlined data set and aiming to delineate a system of stochastic connections between NAO and AMF, a three block matrix was designed containing data on daily NAO, rainfall and flood magnitude. Each row i of the matrix (containing n rows) refer to an AMF event (Fig. 2). This data model can be viewed as the concatenation of three blocks of contingency tables, where each one cross-tabulates the annual maximum flood event with variables related to NAO (block 1), rainfall (block 2) and flood magnitude (block 3). The first block, referring to NAO, display the concatenation of eight two-way (NAO+ and NAO−) contingency tables, each one providing, for the set of individuals (AMFs), the absolute frequency of both positive and negative NAO mode days (i.e. number of days of each mode) within 5-day intervals (Fig. 2), during the 40 days previous to AMF they refer to. The second block indicates the total rainfall accumulated in each 5-days interval (total of 8 columns), and can be viewed as a $n \times 8$ contingency table, in which the absolute frequency is expressed by rainfall (in mm) and n is the total number of AMFs or rows. Each element of this contingency table provides the counts of each rainfall event, being the unit to account for rainfall frequency given by 1 mm. The third contingency table is a classic indicator matrix, displaying the value 1 for the modality corresponding to the flood category (from centennial to ordinary floods) assigned to each AMF, and 0 to the others.

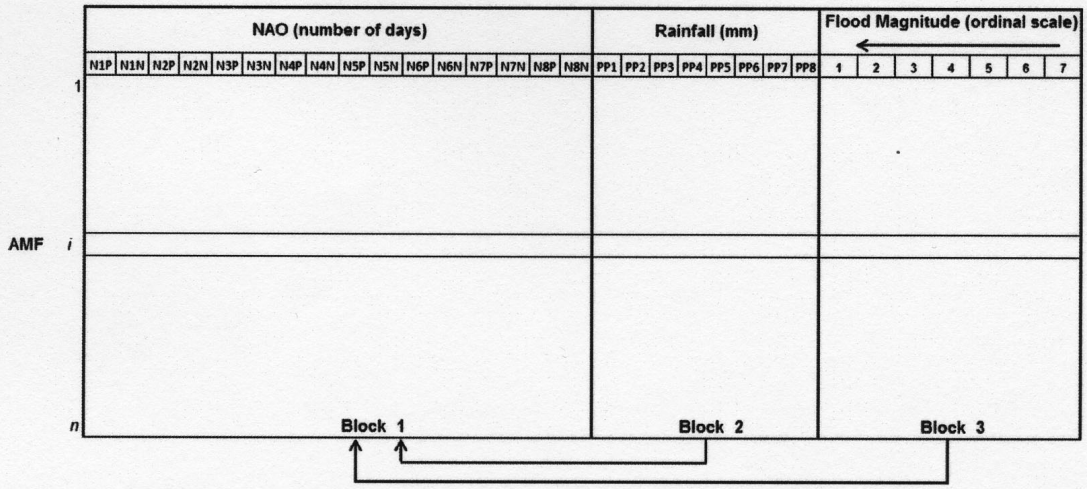

Fig. 2. Data model contingency tables. Block 1: number of days with positive (+) and negative (−) NAO index within 5-day intervals. Block 2: rainfall accumulated for each 5-day intervals. Block 3: flood magnitude category.

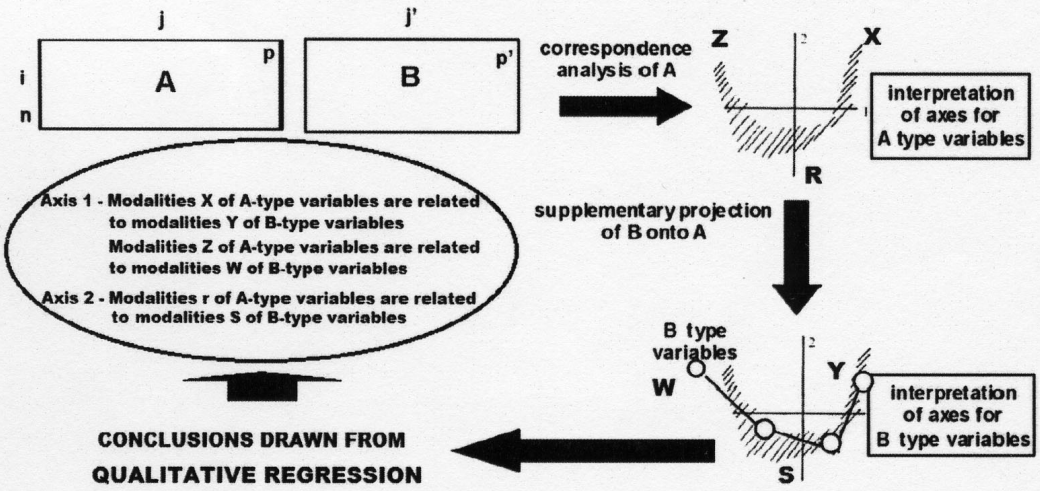

Fig. 3. Outline of the procedure to use CA as a qualitative regression tool.

3.2. Correspondence Analysis

The appropriate multivariate statistical method to deal with contingency tables is Correspondence Analysis (CA), as put forward by Benzécri (1973), and disseminated by Greenacre (2007). This is a very powerful method that can be used as a qualitative non-linear regression tool with predictive capabilities, as it was demonstrated in Salgueiro et al. (2008), and developed in this paper along the same lines.

The crucial step to provide a CA based qualitative regression is the *supplementary projection* of dependent variables (in this case, the Rainfall and Flood magnitude category blocks, as illustrated in Fig. 2) onto the axes produced by the eigenvalue decomposition of the active block referring to predictors (in this case, the NAO block). The supplementary projection is a specific tool Correspondence Analysis, providing, in graphical form, the relationship between variables and the eigenvectors (axes) derived from the active block. As expected from the specific nature of model involving contingency tables, qualitative regression does not yield an equation relating dependent variables, denoted B in Fig. 3, with predictors, denoted A in the same Figure. However, as the projections of each modality of B-type variables onto the relevant axes extracted from the active block are related to A-type variables through their coordinates, the axes mediate a qualitative regression in graphical terms, as illustrated in Fig. 3.

In addition to the graphical display given in Fig. 3, it is worth noting that CA provides an objective criterion to select which A-type variable modalities are related to each axis (X and Z for axis 1 and R for axis 3). This decision is based on the Absolute Contribution of each modality j of A-type variables to the relevant axis, given by the % of the axis total variance conveyed by modality j, as expressed below:

$$C_{j\alpha}^{a} = \frac{f_j f_{i\alpha}'^2}{\lambda_\alpha} \times 100 \tag{1}$$

where $f_j = \frac{K(j)}{K} K(j)$ being the sum of column j, K the sum of the p columns and λ_α the eigenvalue assigned to axis α.

If the modalities were randomly dispersed around the axis, the Absolute Contributions assigned to each of them would be $100/p$. Thus, the criterion for deciding which A-type variable modalities are to be used to interpret an axis is to impose a threshold of $100/p$ in their Absolute Contributions.

As for supplementary variables, no theoretical criterion is available to select modalities linked to a given axis. Nonetheless, once chosen the relevant axes, the criterion to select which modality is linked to each axis relies simply on the inspection of Relative

Contributions, as given below, and assigning the modality with the axis which Relative Contribution exceeds the practical threshold of 0.01, based on similar cases.

$$C_{\alpha j''} = \frac{f_{j''\alpha}^{\prime 2}}{\rho^2}, \text{ with } \rho^2 = \sum_{\alpha} f_{j'\alpha}^{\prime} \quad (2)$$

where $f'_{j'\alpha}$ is the projection of supplementary column j' onto axis α.

In Fig. 3, the above given criteria lead to select W and Y as modalities linked to axis 1 and S, to axis 2. Hence, the conclusions drawn from qualitative regression can be summarized in the relationships $Y \rightarrow X$, $W \rightarrow Z$, $S \rightarrow R$ (where $\rightarrow$ stands for "depends on"), omitting the axes that mediate them, and using only the original variable modalities.

4. Results

4.1. Descriptive results of the model relating flood magnitude with frequency of NAO mode in five days periods

Correspondence Analysis results, obtained by applying the algorithm to the previously described data base model (Fig. 2), can be visualized in Fig. 4, in the plan spanned by Axes 1 and 2. These axes were constructed taking into account only the active variables referring to block (1) of Fig. 2, which can be viewed as a series of eight two way contingency tables, cross-tabulating the AMF events with NAO index mode, within continuous 5-days periods. By projecting blocks (2) and (3) as supplementary variables onto the axes provided by block (1), a relationship between the supplementary and active variables was obtained.

The labels associated to each variable modality, plotted in Fig. 4, where chosen following the procedure given bellow:

(1) In what NAO modalities are concerned, labels are given by NxP or NxN, being x the ordinal denoting the 5-days period prior to applicable AMF (N1P is the first 5-days period for positive NAO, N2P, the second, etc., and the same notation was used for negative NAO, applying the code N after the ordinal, N1N, N2N, etc.).
(2) Regarding rainfall modalities, labels are given by PPx, x denoting the same ordinal as in (1).

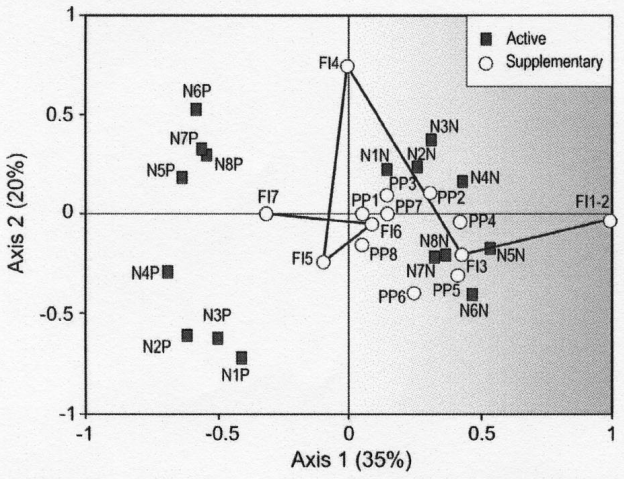

Fig. 4. Projection of NAO modalities onto Axes 1 and 2 derived by CA application to block (1) (squares) and supplementary projections of rainfall and flood magnitude modalities onto Axes 1 and 2 (circles). Note that negative values of NAO (NxN) and the largest flood categories (FI1-2, FI3) are projected onto the right semi-axis 1 (reddish background) whereas on the left semi-axis 1 are projected modalities associated with positive NAO index (NxP) and small flood categories (FI7, FI5).

(3) Flood magnitude classes 1 and 2 (as given in Table 1) were aggregated into one single category (FI1-2) to ensure a minimum of statistical significance. The ordinal y contained in FIy stands for categories described in Table 1.

The plot of Fig. 4, explaining 55% of the information contained in the input table, is interpreted in terms of the meaning of their axes as follows:

- Axis 1 (explaining 35% of the total information) separates clearly positive values of NAO index projected onto its left side, from the negative values of the same variable, which project onto the right semi-axis. In addition, applying the CA criterion that establishes a threshold in the Absolute Contribution of a column to an axis as $100/p = 6.25$ (where $p = 16$ is the number of active columns in Fig. 2), the variables retained as significant for the left part of Axis 1 are N4P, N5P, N7P, N8P; conversely, columns N4N and N5N are retained for the interpretation of the right part of Axis, according to Absolute Contributions given in Table 2 (whenever the absolute contribution of a given modality for the two axes exceeds the threshold, this modality is assigned to the axis for which its absolute contribution is greater, as depicted in Table 2 in bold).
- Axis 2 (explaining 20% of the total information) splits variables N3N and N6P (which project onto its upper part) from variables N1P, N2P, N3P and N6N (which project onto the negative semi-axis).
- N1N, N2N, N7N and N8N are no interpretable in this plane, since their Absolute Contribution is not significant (being less than 6.25, both for Axis 1 and 2, as seen in Table 2).

Considering now Fig. 4 in what supplementary variable FI (flood magnitude) is concerned, a trend on such a variable can be noticed: the flood magnitude grows from left to right, along Axis 1. However, the examination of the Relative Contributions (Table 3) of Flood Magnitude's categories to Axis 1 brings on the conclusion that only FI7 (minor flood, projected onto the left semi-axis 1), FI3 (exceptional flood, T 25–50 years, projected onto the right semi-axis 1), and FI1-2 (centennial to rare floods, $T > 50$ years, projected on the extreme Axis 1 right part) are linked to some extent with Axihs 1. Similarly, it can be stated that all the other intermediate modalities of FI do no relate to Axis 1.

Hence, combining the interpretation of Axis 1 in terms of NAO modalities with the selected significant modalities of FI, it can be established that FI7 ($T \sim 2$ years) is associated with a high occurrence of positive NAO days, namely N4P, N5P, N7P and N8P.

Table 2
Absolute Contributions for NAO active modalities (relevant modalities for each axis depicted in bold).

	Axis 1	Axis 2
N1P	2.4948	**12.8748**
N1N	0.8015	4.1632
N2P	6.8401	**10.9711**
N2N	2.7876	4.4881
N3P	5.8700	**15.1097**
N3N	3.5942	**9.2840**
N4P	**10.9769**	3.1345
N4N	**6.6779**	1.9125
N5P	**11.2194**	1.7350
N5N	**9.4091**	1.4570
N6P	8.7203	**12.3740**
N6N	7.4071	**9.0151**
N7P	**7.4485**	4.4618
N7N	3.8326	2.7948
N8P	**7.1473**	3.7565
N8N	4.7744	2.4692

Table 3
Relative Contributions of the modalities projected supplementary (relevant modalities for each axis depicted in bold).

	Axis 1	Axis 2
PP1	0.0068	0.0011
PP2	**0.0847**	0.0153
PP3	**0.0107**	0.0061
PP4	**0.0730**	0.0002
PP5	**0.0738**	0.0370
PP6	0.0305	**0.0759**
PP7	0.0084	0.0001
PP8	0.0011	0.0079
FI12	**0.0749**	0.0000
FI3	**0.0178**	0.0033
FI4	0.0000	**0.0499**
FI5	0.0021	**0.0108**
FI6	0.0023	0.0003
FI7	**0.0532**	0.0001

Regarding FI3 and FI1-2, these modalities are only associated with N4N and N5N.

As for Axis 2, FI4 (extraordinary flood, T 10–25 years) is (strongly) linked to the positive semi-axis 2 (being associated with N3N and N6P) and FI5 are (weakly) linked to the negative semi-axis 2 (although their association with NAO variables is not reliable). Consequently, given the small frequency (9 events) of FI4 occurrences and the unreliable association of FI5 with NAO modalities (due to weak Relative Contributions), it can be inferred that Axis 2 is not prone to interpretation, in terms of a putative relationship between NAO and FI.

As far as the relationship between Rainfall and NAO is concerned, it can be suggested that PP2, PP3, PP4 and PP5 relate with negative NAO values (mainly N4N + N5N) through their supplementary projections onto Axis 1, and PP6 relates with N1P + N2P + N3P + N6N, through Axis 2 (see Table 3).

On the other hand, no evidence can be drawn from Fig. 4 in relation with the intermediate floods and their connection with NAO (except for FI4, whose relationship with N6P + N3N is nevertheless jeopardized by its negligible number of occurrences).

As a summary, the results of CA for building a descriptive model of the qualitative relationship between Flood Magnitudes, Rainfall and frequency of NAO modes in five days periods can be summarized by stating that the only significant associations found are:

- Centennial to Exceptional Floods (FI1-2 and FI3) are associated with NAO negative phases N4N and N5N, as well as to PP2 + PP3 + PP4 + PP5;
- Minor Floods (FI7) are associated only with NAO positive phases, namely N4P + N5P + N7P + N8P.

Also, given the statistical irrelevance of the association between any category of flood magnitude and the first, second and third NAO periods (positive or negative), it can be stated that the influence of NAO on AMF shows evidence of a minimum delay of 15 days.

4.2. Dam regulation effects on the relationships of flood magnitude with daily NAO patterns

Previous analysis covered the entire set of flood episodes since 1852 without considering the effects of streamflow regulation by dams on the annual maximum flood records. A point that can be addressed is how this flow regulation mainly after the 1960s has modified the natural flood-NAO relationship.

Current reservoir storage capacity at the Tagus basin at the Spanish territory is ca $14{,}500 \times 10^6\ m^3$, higher than the average annual water resource volume estimated in $10{,}853 \times 10^6\ m^3$ (MIMAM, 2000). In 1950, the reservoir storage capacity was only $388 \times 10^6\ m^3$, but increased by 1960 to $4175 \times 10^6\ m^3$ and in 1970 to $6958 \times 10^6\ m^3$. The largest reservoirs Entrepeñas-Buendia ($2394 \times 10^6\ m^3$) were built in 1956–1958, the Alcántara I ($1020 \times 10^6\ m^3$) in 1946 and the Alcantara II ($3160 \times 10^6\ m^3$) in 1969. A cutting date of 1960 was selected for the analysis of the reservoir effect in altering natural NAO impact on flood response.

In order to elucidate the dam effects on NAO-flood relationships, the data matrix represented in Fig. 2 was split into two sets of rows: the first refers to AMFs that occurred before 1959 (denoted Pre), and the second, denoted Post, contains the remaining (post-1960) cases. These two sets of rows were arranged under a matrix form to be independently submitted to the CA algorithm, projecting Flood Magnitudes and Rainfall modalities as supplementary variables onto the Axes provided by the NAO block. The results of these analyses are shown in Figs. 5 and 6, which are interpreted in the sequel focusing on the extreme values of Flood Magnitude (note in Fig. 6 that the class FI4 of intermediate floods – $T \sim$10–25 years – does not occur in matrix Post). Significant values of NAO modalities were selected in both cases by the usual threshold criterion (Absolute Contribution >100/16 = 6.25 – Table 4). Relative Contributions of supplementary modalities are presented in Table 5.

When comparing plotted NAO modalities associated with different flood magnitudes, prior and post-dam construction, it can be deduced that, for the matrix Pre, the modalities of NAO associated with the largest floods (FI1-2) are N5N and N7N, while for Matrix Post, N4N, N5N and N6N are associated with the same flood category.

In the case of exceptional floods (FI3), the significant modalities of NAO are N5N and N7N for matrix Pre (linked to axis 1), while for Matrix Post, N1P, N2P and N3P (linked to axis 2) are associated with the same flood category.

In the case of small AMFs, the influence of positive NAO is made with N2P, N4P, N5P, N7P and N8P (linked to axis 1) for matrix Pre, whereas for Post, the association is made with N4P, N5P and N8P (linked, also, to axis 1).

Regarding Rainfall relationships, for matrix Pre, PP1, PP2, PP4 and PP5 are associated with FI1-2 and FI3; whereas for matrix Post the association is made with PP4, PP5 and PP7, only for FI1-2.

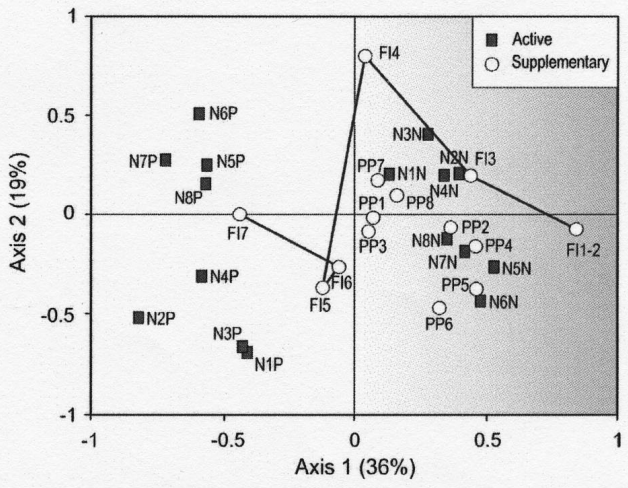

Fig. 5. Supplementary projection of Flood Magnitudes on Axis 1 and 2 provided by NAO modalities, using a matrix with flood events that occurred before dam regulation at the Tagus River catchment (matrix Pre, flood occurrence before 1960). All flood categories are represented following a line from smaller floods, plotted at the left side, to the largest flood categories projected on the right semi-axis 1.

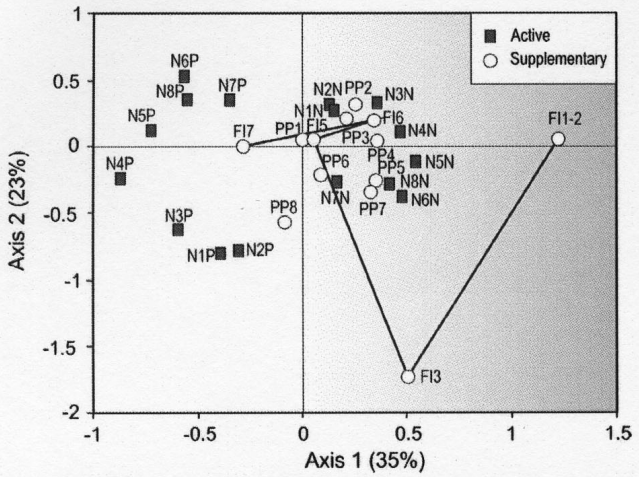

Fig. 6. Supplementary projection of Flood Magnitudes on Axis 1 and 2 provided by NAO modalities, using a matrix with flood events that occurred after dam regulation of the Tagus River catchment (matrix Post, flood occurrence after 1960). Note that intermediate flood category FI4 (return interval $T \sim 10$–25 years) has disappeared in this matrix due to complete flood peak attenuation by reservoirs.

Table 4
Absolute Contributions for NAO active modalities for matrices Pre and Post (relevant modalities for each axis depicted in bold).

	Matrix Pre		Matrix Post	
	Axis 1	Axis 2	Axis 1	Axis 2
N1P	2.3663	**11.7432**	2.4679	**14.6033**
N1N	0.7394	3.7097	0.8227	4.8676
N2P	**11.2928**	8.4207	1.7338	**15.4555**
N2N	4.6448	3.4803	0.6996	**6.2359**
N3P	4.039	**17.7882**	8.1388	**12.5198**
N3N	2.5741	**11.4112**	4.7124	**7.2493**
N4P	**7.6998**	3.9599	**16.0613**	1.5724
N4N	5.2424	2.7098	**8.335**	0.8159
N5P	**8.8268**	3.627	**13.7795**	0.6997
N5N	**8.2176**	3.3876	**10.0139**	0.5086
N6P	8.8982	**12.7652**	7.8281	**10.9145**
N6N	6.9632	**10.026**	**7.7337**	**7.0387**
N7P	**10.8235**	3.2524	3.0826	4.9027
N7N	**6.3104**	1.9026	0.8973	3.4277
N8P	**6.9844**	1.1277	**7.9301**	5.3214
N8N	4.3772	0.6884	5.7631	3.8672

Table 5
Relative Contribution of the modalities projected supplementary for matrices Pre and Post (relevant modalities for each axis depicted in bold).

	Matrix Pre		Matrix Post	
	Axis 1	Axis 2	Axis 1	Axis 2
PP1	**0.0201**	0.0000	0.0029	0.0081
PP2	**0.1029**	0.0030	0.0630	**0.1129**
PP3	0.0012	0.0014	0.0285	**0.0373**
PP4	**0.0810**	0.0091	**0.0528**	0.0013
PP5	**0.0722**	0.0422	**0.0683**	0.0291
PP6	0.0572	**0.1105**	0.0030	**0.0179**
PP7	0.0040	0.0150	**0.0425**	**0.0424**
PP8	0.0118	0.0059	0.0032	0.1227
FI12	**0.0591**	0.0002	**0.0991**	0.0005
FI3	**0.0260**	0.0066	0.0106	**0.1263**
FI4	0.0003	**0.1091**	–	–
FI5	0.0042	**0.0359**	0.0000	0.0006
FI6	0.0013	**0.0195**	**0.0291**	0.0124
FI7	**0.0433**	0.0001	**0.1153**	0.0007

4.3. Predictive capability of the model in forecasting future floods

Several authors have studied the potential of the NAO index as a predictor of winter precipitation in the western part of the Iberian Peninsula (Zorita et al., 1992; Corte-Real et al., 1998; Rodó et al., 1997; Rodríguez-Puebla et al., 2001; González-Rouco et al., 2000; Trigo and Palutikof, 2001; Trigo et al., 2004). Developing such capability of the North Atlantic circulation as predictor of hydro-climatic variables represents a great challenge, and a potential tool for the water sector, including water resource management, hydropower generation and flood mitigation. Here, we intend to explore how sequential patterns of daily NAO index can provide insight into this predictive capability to anticipate large floods in the Tagus River.

Results obtained in Section 4.1 allow to use the CA based qualitative regression model as predictive device to forecast extreme floods. In fact, if we rearrange Fig. 4 by representing only the variables' modalities that were considered significant on the grounds of the case made in Section 4.1 by considering Absolute and Relative Contributions to Axis 1, we can sketch the plot of Fig. 7, where the above given interpretation can be visualized.

In fact, the final summary conclusions established in Section 4.1 are made clearer by their graphical representation in Fig. 7, which can be used as a predictive tool in forecasting future floods for a new event that is not contained in the training set.

From the examination of the left side of Fig. 7 (negative semi-axis 1), it can be deduced that a 'gentle' annual maximum flood (FI7, minor flood) occurs during years with dominant positive NAO index, whenever occurs a period of 20 days where NAO is predominantly positive.

From the examination of the right side of Fig. 7 (positive semi-axis 1), the conclusion is drawn that an intense flood (FI3 or FI1-2) is expected to arise 15 days later, whenever occurs a period of 10 days where NAO is predominantly negative.

The above presented predictive capabilities of the model were based on the entire set of events contained in the data base. The question can be put if the model responds in the same way for the post-dam period (from 1960 onwards, containing only 48 out of 113 years). The affirmative answer to that question can be deduced from the comparison of Fig. 7 with Fig. 8, where Fig. 5 – referring to the post-dam period – was rearranged to include only the significant modalities of the variables (as in Fig. 7).

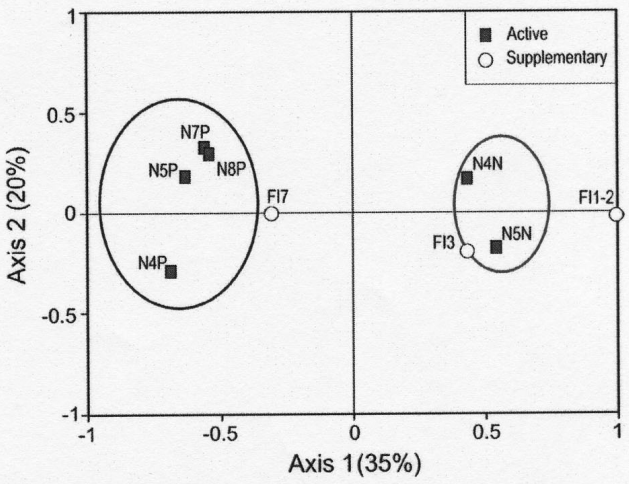

Fig. 7. Plot of significant NAO and Flood magnitude modalities (the blue ellipse bounds positive NAO modalities linked to small floods (FI7) while the red one bounds the negative NAO modalities linked to large floods (FI1-2 and FI3). The positive semi-axis 1 (right side) shows that large floods (FI3 and FI1-2) which are associated with a 10-days period (N4N and N5N) with predominant negative NAO.

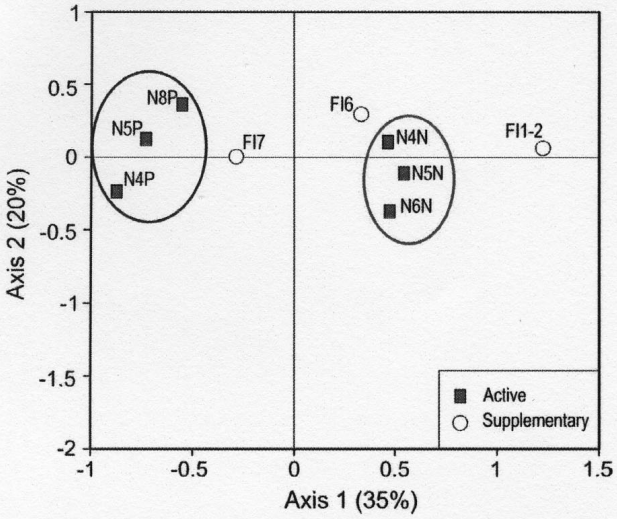

Fig. 8. Plot of significant NAO and Flood magnitude modalities for the post-dam period (1960 onwards). Despite of river regulation, large floods (FI1-2) have occurred over the post-dam period although requiring a longer period of time with a negative NAO mode (15-days, N6N, N5N and N4N).

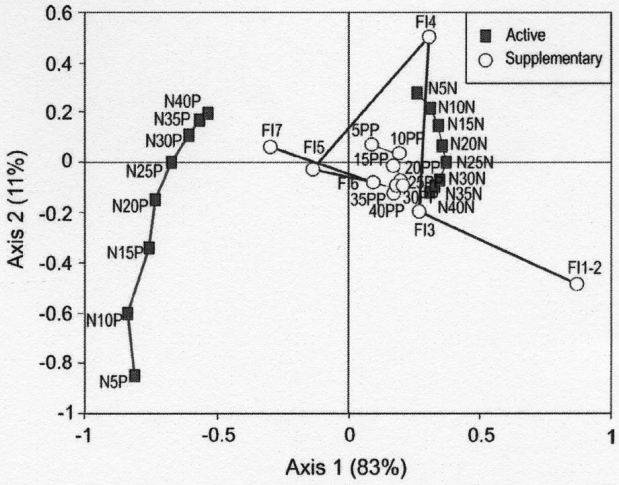

Fig. 10. Projection of NAO modalities into Axes 1 and 2 derived by CA application to block (1) of the aggregate data model (squares) and supplementary projections of rainfall and Flood Magnitude (circles). The largest accumulate rainfall amounts related with the longest negative NAO modes. Large floods (FI1-2) related with all periods of negative NAO.

In fact, the same general configuration is illustrated in Fig. 7 and 8, which validates the predictive capabilities of the model to forecast future floods, according to the rules deduced from Fig. 7 for a larger set of events (113 cases).

4.4. Assessment of the model by interpreting misclassified cases for cumulative data

In order to assess the robustness of the analysis, a test was conducted with an aggregate data model (Fig. 9). In this model, the occurrence of positive and negative values of daily NAO are accumulated in periods of 5–40 days prior to each AMF (N5P to N40P, and N5N to N40N, for periods of positive and negative NAO modes).

The meaning of the labels of the CA plot presented in Fig. 10 (and its correspondence with Fig. 9 data model) is explained below:

(1) As for NAO modalities, the labels are N*x*P and N*x*N, where *x* stands for the number of days accumulated with positive and negative NAO, respectively, before the appropriate AMF.
(2) Regarding Rainfall, the labels are *x*PP, where *x* has the same meaning as in 1)

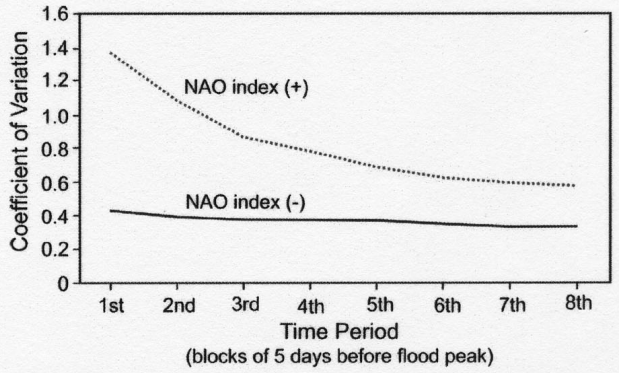

Fig. 11. Coefficient of variation for positive and negative NAO aggregated periods. Note that the coefficient of variation for positive NAO index is higher and increases towards the time of flood peak. Negative NAO associated to large flooding shows a minor difference of its coefficient of variation.

(3) The labels for AMFs are the same as given in Section 4.1 for Fig. 4.

The graph produced by the CA application to Fig. 9 block (1) as active is shown in Fig. 10, where Axis 1 separates positive from negative NAO, as expected. Fig. 10 also displays the supplementary

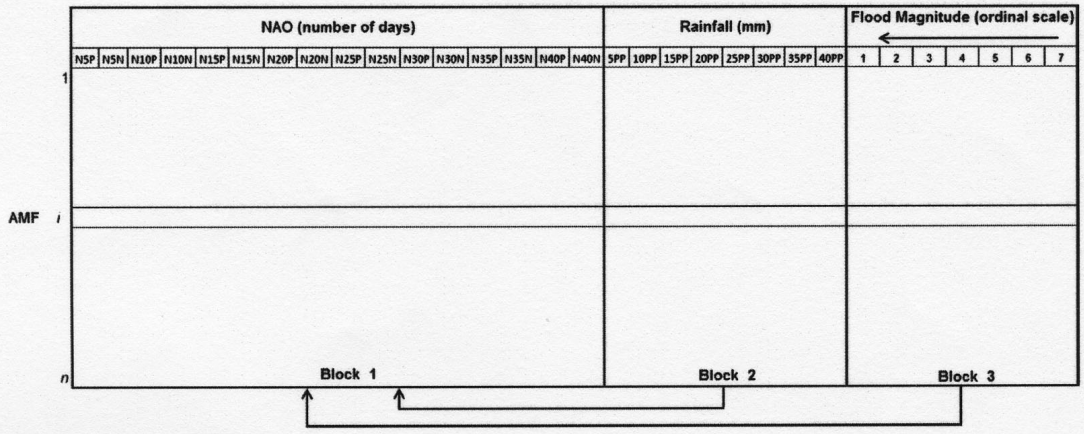

Fig. 9. Aggregate data model.

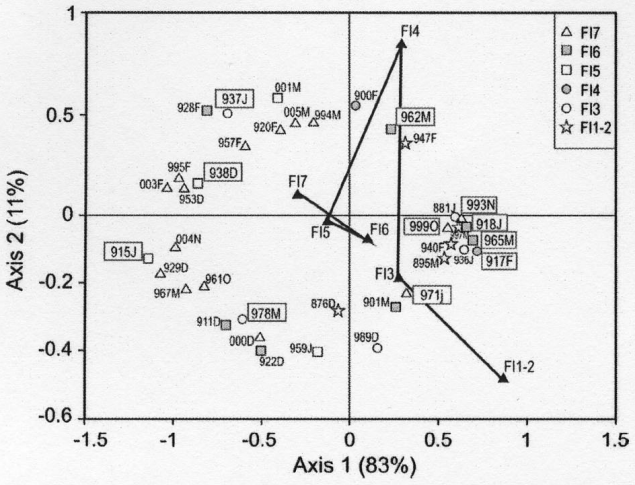

Fig. 12. Projection of AMFs onto the principal CA plane, drawing attention to the two types of outlier cases (red boxes correspond to severe floods that project onto the left part of axis 1, characterized by small floods and green boxes to the reverse).

projections of Flood Magnitude (FI) and Rainfall (*x*PP) onto the axes created by block (1). It is worth noting that the sequence of positive NAO projections spreads along axis 2, in contrast with negative ones, which cover a limited region of the graph (bounded roughly by co-ordinates in Axis 2 of −0.2 and 0.2. This can be explained by the analysis of Fig. 11 where the coefficient of variation for positive and negative NAO aggregated periods is plotted against such periods.

The main conclusions drawn from the plot represented in Fig. 10 are the following:

- Large flood magnitude categories (FI1-2) are related with all periods of negative NAO, while small flood magnitudes (FI7) do not depend on the time-length of NAO modality (but only on the fact that they exhibit a positive NAO mode). The intermediate flood categories do no relate univocally with the separation from positive to negative NAO occurrences.
- Rainfall relates directly with negative NAO according to the sequence of the latter in axis 2. This relation points out, once again, to the critical role of NAO on precipitation, and how accumulated precipitation drives the occurrence of floods.

On the whole, it can be stated that the interpretation of the aggregate data model leads to conclusions noted already by previous work linking large floods with persistent negative NAO mode (Paredes et al., 2006; Trigo et al., 2008; Benito et al., 2008; Trigo, 2011; Lorenzo-Lacruz et al., 2011). Such an interpretation does not improve expressively the understanding of these NAO-flood relationships for the intermediate flood categories.

Finally, in order to improve the understanding of the almost trivial conclusions drawn from Fig. 10, the CA property that allows the simultaneous projection of individuals and properties onto the same graph was put into practice, by projecting rows of the matrix plotted in Fig. 9 onto the same axes obtained in Fig. 10.

A more clear graphic representation of the results was obtained by plotting in Fig. 12 only the significant individuals which were selected by imposing the usual threshold of $100/n$ in the Absolute Contributions to Axes 1 and 2, where n is now 113.

The point to be addressed by this experiment is meant to elucidate how individuals (AMF) distribute for the extremes of Axis 1, corresponding to the largest (right semi-axis 1) and smaller (left semi-axis 1) Flood Magnitudes. This analysis is focused on misclassified cases, i.e., individuals (denoted I in Table 6) that do not follow the general rule regarding the presence of a negative NAO mode, or number of days required with a negative phase, and the occurrence of high AMFs, and conversely, the relation between the presence and time length of a positive NAO mode, and the occurrence of low magnitude floods (denoted II in Table 6). In Fig. 12, misclassified individuals are highlighted trough boxes surrounding their labels (red boxes correspond to I type cases and green ones to II type misclassified cases).

Three main causes can be suggested from the rainfall and hydrological analysis of the misclassified cases (Table 6) that can explain their phenomenological behaviour: (i) human-induced, (ii) soil hydrological characteristics associated to wet hydrological years and, (iii) rainfall patterns in normal/dry climatological years.

Table 6
Explanation of misclassified cases and type of outlier flood events. Type I: Projected onto the negative Axis 1. Type II: Projected onto the positive Axis 1.

Flood magnitude category	Date	ID code	Misclassification type	Explanation
Rare (3) (8000–10000 $m^3 s^{-1}$)	31/01/1937	937J	I	Wet Autumn and Winter, following a very wet year. High soil moisture. Response to 8 days uneven distributed rainfall
	21/03/1978	978M	I	Water released by dam operation
Extraordinary (4) (6000–8000 $m^3 s^{-1}$)	12/02/1917	917F	II	Wet Autumn and Winter. Saturated soils. Flood was produced following a two high intensity rainfall events (<72 h) within a 5-day interval
Occasional (5) (4000–6000 $m^3 s^{-1}$)	04/01/1915	915J	I	Saturated soils, after a wet Autumn/early Winter. Flood occurring after a 5 day rainfall distribution pattern, typical of minor magnitude floods (50 mm accumulated rainfall)
	12/12/1938	938D	I	Hydrological behaviour, and rainfall pattern-accumulated volume, identical to previous event (915 J)
Ordinary (6) (2000–4000 $m^3 s^{-1}$)	09/01/1918	918 J	II	Dry autumn but wet December. A total of 104 mm within a 8-day interval produced by 2 short-lived (48 h) high intensity rainfall events
	09/03/1962	962M	II	Dry autumn but wet Winter. 130 mm accumulated within a 15 days interval, but with a very discontinuous intensity, with most of the precipitation falling in 3 (24 h) events (25 to 43 mm), within a 2–3 day interval.
	02/03/1965	965M	II	Water released by dam operation
Minor (7) (<2000 $m^3 s^{-1}$)	02/07/1971	971j	II	Water released by dam operation
	03/11/1993	993N	II	Dry hydrological year. Flood occurring after a 6 days continuous rainfall (61 mm) with an even daily distribution, under a 5 days positive NAO
	24/10/1999	999°	II	Dry hydrological year. Flood occurring after a 8 days uneven rainfall daily distribution (rainfall events over, 20 mm/24 h, in alternating days), with a total accumulated rainfall of 112 mm, under low strength signal negative NAO

(i) Misclassified cases identified as 978M (exceptional flood), 965M (ordinary) and 971j (minor), do not have a natural cause. These floods were generated by the release of stored water during dam operations.
(ii) The exceptional magnitude flood of 1937 (return period of 50 years), and the extreme (1917) and extraordinary magnitude floods of 1915 and 1938 were generated within a time length period of consecutive negative NAO index days inferior to the pattern resulting from the CA application. The presence of saturated soils, recharged aquifers and high seasonal base flow made possible the fast hydrological response to short-lived rainfall events, taking place within a week.
(iii) Misclassified cases for the floods occurring in dry years (or in years with a higher seasonal variability) indicate their sensitivity towards the rainfall daily pattern distribution, which relates to the number of continuous positive or negative NAO index days as well as the signal strength.

5. Discussion and conclusions

Flood generation in the Tagus River (catchment surface of 80,600 km^2), as in other major Iberian rivers, is associated with wide ranging and continuous precipitation (over several weeks), mainly occurring during winter months, giving rise to flood hydrographs lasting for 4–7 days. The seasonal and inter-annual variability of this winter rainfall is strongly controlled by the North Atlantic circulation pattern (Zorita et al., 1992; Rodó et al., 1997), with high (low) seasonal river flow being associated with negative (positive) phase of the NAO (Trigo et al., 2004; 2011). Regarding floods, years with large floods or with higher number of floods tend to occur when the NAO is in negative phase (Benito et al., 2005; 2008; Silva et al., 2012).

In order to perform a detailed analysis of the dependence of the annual peak discharge from the North Atlantic circulation mode, it is required a thorough analysis of the antecedent values of NAO index at a daily scale. This is precisely the basis for this study, focussed on the Correspondence Analysis based data treatment of NAO mode and rainfall volume during the 40 days previous to the maximum annual flood peak at the lower Tagus River. A qualitative regression procedure – relying on supplementary projection of rainfall and flood magnitude onto the Correspondence Analysis axes provided by NAO mode modalities – was applied to seven flood categories in relation with the accumulated number of days with negative (positive) NAO days and precipitation volume in eight groups of five days previous to the date of the flood occurrence.

The Correspondence Analysis results show a clear association between the 40 days antecedent NAO mode and flood magnitudes for the largest and smallest flood categories. The largest floods (return period equal and over 25-years) occurred when a negative NAO dominated over a period of 10 days, starting at least 25 days prior to the peak. For small floods (recurrence interval $T < 2$ years) a positive NAO index prevailed over a 2 periods of 10 days with a lag of 15 and 30 days. These results are in agreement with the general pattern linking average (seasonal) NAO phase during winter months with total volume of winter precipitation (Corte-Real et al., 1998) that drives into large floods over historical-instrumental periods (Benito et al., 2008) and gauge records (Silva et al., 2012).

This relationship between NAO mode and flood magnitude is more complex for intermediate flood categories. The number of exceptions and the lack of univocal statistical association between the persistence of NAO phase and occurrence of the intermediate floods, once again demonstrate the nonlinearity of the hydrological response to NAO, and dependence of seasonal weather and antecedent catchment conditions (Trigo et al., 2004; López-Moreno et al., 2007). Thus, previous studies analysing seasonal or monthly NAO index values on flood magnitude failed to reach robust conclusions for intermediate flood magnitudes (e.g. Silva et al., 2012). The improvement brought by Correspondence Analysis (CA) to this ambiguous situations refers to intermediate floods of category FI3 (T: 25–50 years), for which a relationship was found between such floods and periods of 10 days of persistent NAO negative mode, with a lag of 15 days.

The CA shows a lack of significant association among large flood categories and NAO index over the previous first, second and third 5-days periods before the flood peak suggesting a 15 day lag time response of flood peaks to daily NAO. As shown by López-Moreno et al. (2007) the lagged response on rainfall stations in relation with NAO phase increases towards the eastern part of the basin, since the cyclonic fronts move from west to east. Here, this 15-day lag response of flood peak to NAO phase is due to the frontal rainfall movement towards the Tagus headwaters (several days, depending on wind speed) and the hydrograph concentration time (time needed for water to flow from headwaters and estimated in 7–8 days). The Correspondence Analysis results confirm the fact that total precipitation tend to increase (decrease) during negative (positive) phases, being such response to NAO phase obviously non- linear. In particular, a period of 20 days, with a lag of 5 days, occurs prior to a centennial to exceptional flood.

Another important result of this study is to show the modification introduced by dam construction and related reservoir operations in the impact of the NAO phase on the flood response. The largest floods (FI1-2) before 1960 (prior to construction of largest Tagus River large dams) were explained by persistent negative NAO phase during two five days periods, with lags of 20 and 30 days, whereas in the post-dam modified record the significant impact of negative NAO mode spreads only for 15 days with a lag time of 15 days. Since most of the large floods tend to occur during wet winters, it may be interpreted that dam operation released an excess of water volume anticipating the "natural" flood peaks which modify the flood hydrograph characteristics. As for small floods, the influence of the positive NAO changed from the entire 40 days period before flood in the pre-dam record (specially with lags of 5, 15 and 35 days), to a narrower period of 10 days in the post-dam period (with a lag time of 15 days). In other words, some of these small floods were artificially induced by the dam operation. Dam management showed the strongest influence on hydrograph peak attenuation in the intermediate flood categories such as exceptional (T ~25–50 years) and extraordinary floods (T ~10–25 years). In the former, for the after dam regime, floods also occurred over a narrower number of days with negative NAO index, whereas the later category almost disappeared of the record due to complete flood peak attenuation by reservoirs. The decrease in the sensitiveness of flood generation to the extreme phases of NAO as a result of increasing regulatory capacity was also detected in relation to monthly streamflow of the Tagus River as well as in other major Atlantic Iberian rivers (Lorenzo-Lacruz et al., 2011).

There are several practical implications of these results on flood hazards of the lower Tagus River: (1) Reservoirs have significantly reduced the influence of negative NAO phase to produce intermediate flood categories (exceptional, T ~25–50 years, and extraordinary floods, T ~10–25 years); (2) Despite of massive river regulation by dams, the largest floods were generated during anomalous wet winters linked to persistent negative NAO phase, and actually associated to a reduced number of days with negative NAO mode (20–35 days negative NAO before 1960 vs. 15–25 days afterwards), most likely favoured by dam operations at basin scale; (3) Flood hazards associated with the largest flood categories should be considered in flood risk management at the lower Tagus River, even if there is a tend to future positive NAO mode as antic-

ipated in several climate change models (Osborn 2004; Kuzmina et al., 2005; Stephenson et al., 2006).

Regarding the methodological conclusions drawn from the CA application to this case study, it seems that some novel results can be offered, and that some improvement in regard to previous studies can be reached, particularly in what concerns the detailed 'explanation' of large floods in terms of well defined periods of persistent NAO negative mode, demonstrating some predictive capabilities of the model. Also, the comparison of flood response to NAO in the pre- and post-dam epochs was made clearer by CA results.

Acknowledgments

This work is supported by the bi-lateral Spanish-Portuguese commission through the project "Temporal analysis of extreme floods in Iberian Rivers in response to North Atlantic Oscillation (NAO) variability" (Portuguese grant E-52/10 and Spanish grant PT2009-0162). Additional support was provided by the Spanish Ministry of Science and Innovation (CICYT) projects GL2008-06474-CO2-01, CGL2011-29176 and PIE-CSIC 200430E595. Instrumental climatological records were provided by the AEMET (Agencia Estatal de Meteorología) and the Icelandic Meterological Office. Gauge records were provided by the INAG (Portuguese Water Agency) and the CEDEX (Centro de Estudios Hidrográficos). We would like to thank to J.I. López-Moreno and A. Assani for their useful comments in the spirit of constructive criticism during the review process.

References

Barriendos, M., Martín-Vide, J., Peña, J.C., Rodríguez, R., 2002. Daily meteorological observations in Cádiz – San Fernando. Analysis of the documentary sources and the instrumental data content (1786–1996). Climatic Change 53, 151–170.

Benito, G., Díez-Herrero, A., Fernandez de Villalta, M., 2003a. Magnitude and frequency of flooding in the Tagus Basin (Central Spain) over the last millennium. Climatic Change 58, 171–192.

Benito, G., Sopeña, A., Sánchez-Moya, Y., Machado, M.J., Pérez-González, A., 2003b. Palaeoflood record of the Tagus River (Central Spain) during the Late Pleistocene and Holocene. Quaternary Science Reviews 22, 1737–1756.

Benito, G., Díez-Herrero, A., Fernández de Villalta, M., 2004. Flood response to NAO and Solar Activity in the Tagus Basin (Cental Spain) over the last millennium. Climatic Change 66, 27–28.

Benito, G., Barriendos, M., Llasat, C., Machado, M., Thorndycraft, V.R., 2005. Impactos sobre los riesgos naturales de origen climático. In: J.M. Moreno (Coordinador), Evaluación preliminar de los impactos en España por efecto del Cambio Climático, Ministerio de Medioambiente, Madrid, pp. 527–548.

Benito, G., Thorndycraft, V.R., Rico, M., Sánchez-Moya, Y., Sopeña, A., 2008. Palaeoflood and floodplain records from Spain: evidence for long-term climate variability and environmental changes. Geomorphology 101, 68–77.

Benzécri, J.P., 1973. L'analyse des données, vol. 2. Dunod, Paris.

Capel, J., 1981. Los Climas de España. Col. Ciencias Geográficas, Oikos-Tau, Barcelona.

Corte-Real, J., Qian, B., Xu, H., 1998. Regional climate change in Portugal: precipitation variability associated with large-scale atmospheric circulation. International Journal of Climatology 18, 619–635.

Cortesi, N., Trigo, R., Gonzalez-Hidalgo, J.C., Ramos, A.M., 2012. High resolution reconstruction of monthly precipitation of Iberian Peninsula using circulation weather types. Hydrology and Earth System Sciences Discussion 9, 6935–6977. http://dx.doi.org/10.5194/hessd-9-6935-2012.

Frances, F., Salas, J.D., Boes, D.C., 1994. Flood frequency analysis with systematic and historical or paleofood data based on the two parameter general extreme value models. Water Resources Research 30 (5), 1653–1664.

González-Rouco, F., Zorita, E., Heyen, H., Valero, F., 2000. Agreement between observed rainfall trends and climate change simulations in the southwest of Europe. Journal of Climate 13, 3057–3065.

Goodess, C.M., Jones, P.D., 2002. Links between circulation and changes in the characteristics of Iberian rainfall. International Journal of Climatology 22, 1593–1615.

Greenacre, M., 2007. Correspondence Analysis in Practice, second ed. Chapman & Hall/CRC, London.

Hurrell, J.W., Kushnir, Y., Visbeck, M., Ottersen, G., 2003. An overview of the North Atlantic Oscillation. In: Hurrell, J.W., Kushnir, Y., Ottersen, G., Visbeck, M. (Eds.), The North Atlantic Oscillation: Climate Significance and Environmental Impact, vol. 134. Geophysical Monograph Series, Washington, DC, pp. 1–35.

Kuzmina, S.I., Bengtsson, L., Johannenssen, O.M., Drange, H., Bobylev, L.P., Miles, M.W., 2005. The North Atlantic Oscillation and greenhouse-gas forcing. G.R.L. 32:L04703. <http://dx.doi.org/10.1029/2004GL021064>.

López-Moreno, J.I., Beguería, S., Vicente-Serrano, S.M., García-Ruiz, J.M., 2007. Influence of the North Atlantic Oscillation on water resources in central Iberia: precipitation, streamflow anomalies, and reservoir management strategies. Water Resources Research 43. http://dx.doi.org/10.1029/2007WR005864.

Lorenzo-Lacruz, J., Vicente-Serrano, S.M., López-Moreno, J.I., González-Hidalgo, J.C., Morán-Tejeda, E., 2011. The response of Iberian rivers to the North Atlantic Oscillation. Hydrology and Earth System Sciences 15, 2581–2597.

Machado, M.J., Benito, G., Barriendos, M., Rodrigo, F.S., 2011. 500 years of rainfall variability and extreme hydrological events in southeastern Spain drylands. Journal of Arid Environments 75, 1244–1253.

MIMAM, 2000. El Libro Blanco del Agua en España. Centro de Publicaciones del Ministerio de Medio Ambiente, Madrid, 637 pp.

Morán-Tejeda, E., López-Moreno, I., Ceballos, A., Vicente-Serrano, S., 2011. Evaluating Duero's basin (Spain) response to the NAO phases: spatial and seasonal variability. Hydrological Processes 25, 1313–1326.

Ortega, J.A., Garzón, G., 2004. Influencia de la oscilación del Atlántico norte en las inundaciones del Río Guadiana. In: Benito, G., Díez Herrero, A. (Eds.), Riesgos naturales y antrópicos en Geomorfología. CSIC, Madrid, pp. 117–126.

Osborn, T.J., 2004. Simulating the winter North Atlantic Oscillation: the roles of internal variability and greenhouse gas forcing. Climate Dynamics 22, 605–623.

Paredes, D., Trigo, R.M., Garcia-Herrera, R., Trigo, I., 2006. Understanding precipitation changes in Iberia in early spring: weather typing and storm-tracking approaches. Journal of Hydrometeorology 7, 101–113.

Rodó, X., Baert, E., Comin, F.A., 1997. Variations in seasonal rainfall in southern Europe during the present century: relationships with the North Atlantic oscillation and the El Niño–southern oscillation. Climate Dynamics 13, 275–284.

Rodríguez-Puebla, C., Encinas, A.H., Sáenz, J., 2001. Winter precipitation over the Iberian Peninsula and its relationship to circulation indices. Hydrology and Earth System Sciences 5, 233–244.

Rossi, F., Fiorentino, M., Versace, P., 1984. Two-component extreme value distribution for flood frequency analysis. Water Resources Research 20 (6), 847–856.

Salgueiro, A.R., Rico, M., Pereira, H.G., Benito, G., Díez-Herrero, A., 2008. Application of correspondence analysis to the assessment of mine tailings dam breakage risk in the Mediterranean region. Risk Analysis 28 (1), 13–23.

Silva, A.T., Portela, M.M., Naghettini, M., 2012. Nonstationarities in the occurrence rates of flood events in Portuguese watersheds. Hydrology and Earth System Sciences 16, 241–254.

Stephenson, D.B., Pavan, V., Collins, M., 2006. North Atlantic Oscillation response to transient greenhouse gas forcing and the impact on European winter climate: a CMIP2 multi-model assessment. Climate Dynamics 27, 401–420.

Trigo, R.M., Palutikof, J.P., 2001. Precipitation scenarios over Iberia: a comparison between direct GCM output and different downscaling techniques. Journal of Climate 14, 4422–4446.

Trigo, R.M., Pozo-Vázquez, D., Osborn, T.J., Castro-Díez, Y., Gámiz-Fortis, S., Esteban-Parra, M.J., 2004. North Atlantic oscillation influence on precipitation, river flow and water resources in the Iberian Peninsula. International Journal of Climatology 24, 925–944.

Trigo, R.M., Valente, M.A., Trigo, I.F., Miranda, P.M.A., Ramos, A.M., Paredes, D., García-Herrera, R., 2008. The impact of North Atlantic wind and cyclone trends on European precipitation and significant wave height in the Atlantic. Annals of the New York Academy of Sciences 1146 (1), 212–234.

Trigo, R.M., 2011. The impacts of the NAO on hydrological resources of the Western Mediterranean. In: Vicente-Serrano, S.M., Trigo, R.M. (Eds.), Hydrological, Socioeconomic and Ecological Impacts of the North Atlantic Oscillation in the Mediterranean Region, vol. 46. Advances in Global Change Research, pp. 41–56.

van Loon, H., Rogers, J.C., 1978. The Seesaw in winter temperatures between Greenland and Northern Europe. Part I: General description. Monthly Weather Review 106, 296–310.

Vaquero, J.M., 2004. Solar Signal in the number of floods recorded for the Tagus River Basin over the Last Millenium. Comment on "Magnitude and frequency in the Tagus Basin (Central Spain) over the last millennium" by G. Benito et al. (2003). Climatic Change 58, 171–192. Climatic Change 66, 27–28.

Vicente-Serrano, S.M., Trigo, R.M. (Eds.), 2011. Hydrological, Socioeconomic and Ecological Impacts of the North Atlantic Oscillation in the Mediterranean Region, vol. 46. Advances in Global Change Research, p. 236 pp.

Walker, G.T., Bliss, E.W., 1932. World Weather. V. Memory Royal Meteorological Society 44, 53–84.

Zorita, E., Kharin, V., Von Storch, H., 1992. The atmospheric circulation and sea surface temperature in the North Atlantic area in winter: their interaction and relevance for Iberian precipitation. Journal of Climate 5, 1097–1108.